Car-Following Behavior Analysis from Microscopic Trajectory Data

Saskia Ossen and Serge P. Hoogendoorn

The development of accurate and robust models in the field of car following has suffered greatly from the lack of appropriate microscopic data. Because of this lack, little is known about differences in car-following behavior between individual driver–vehicle combinations. This paper studies the car-following behaviors of individual drivers by making use of vehicle trajectory data extracted from high-resolution digital images collected at a high frequency from a helicopter. The analysis was performed by estimating the parameters of different specifications of the well-known Gazis–Herman–Rothery car-following rule for individual drivers. This analysis showed that a relation between the stimuli and the response could be established in 80% of the cases. The main contribution of this paper is that considerable differences between the car-following behaviors of individual drivers could be identified. These differences are expressed as different optimal parameter values for the reaction time and the sensitivity, as well as different car-following models that appear to be optimal on the basis of the data for individual drivers.

Microsimulation models play an important role in the analysis of existing traffic facilities needing modification and also in the design of new facilities. It is therefore of great importance to make sure that these simulation models are able to simulate real traffic situations sufficiently well. One important subprocess in microsimulation models consists of the modeling of car-following behavior.

Although this special kind of behavior has been the topic of much research in the past [an overview has been provided elsewhere (*1*)], the development of accurate and robust models has suffered greatly from the lack of appropriate microscopic data. Car-following theories and models are generally based on small-scale observations and experiments that have been conducted many years ago or with observed flow data, which provide information only at an aggregate level (1- or 5-min averages) and at a limited number of cross sections. Furthermore, little is known about differences in car-following behavior between individual driver–vehicle combinations, also because of the lack of detailed microscopic traffic data.

This paper forms a starting point for new research in the field of car following. This research, however, focuses not only on the analysis of car-following behavior but also on the development of a new data collection method based on remote sensing (*2*). The development of this method enables the use of detailed trajectory data derived from pictures taken with a digital camera attached to a helicopter. As these pictures are taken at regular intervals of 0.1 s, they provide extensive information about the movements of vehicles.

Transport and Planning Department, Faculty of Civil Engineering and Geosciences, Delft University of Technology, P.O. Box 5048, NL-2600 GA, Delft, Netherlands.

Transportation Research Record: Journal of the Transportation Research Board, No. 1934, Transportation Research Board of the National Academies, Washington, D.C., 2005, pp. 13–21.

The aim of this paper is to answer the following research questions:

1. Can the car-following behaviors of individual drivers be adequately described by using relatively simple car-following models?
2. Is driver behavior conceptually similar for individual drivers, in the sense that the same car-following model can be used?
3. What is the variability in the car-following behaviors of individual drivers?

The answers to these research questions will be obtained by using one of the first data sets to examine a well-known stimulus–response model: the Gazis–Herman–Rothery (GHR) model. Three special cases of the GHR model are calibrated for all observed leader–follower combinations separately by performing least-squares estimations. That is, an individual car-following model has been estimated from the trajectory data for each driver–vehicle combination.

The estimation results enable not only investigation of whether relationships exist between the acceleration and the stimuli given by the models but also comparison of the optimal values for the sensitivity parameter c and the reaction time T_r between individual drivers in case of a relationship. The results of the different models are also compared to identify whether one model outperforms the other models.

DESCRIPTION OF TRAJECTORY DATA

Many different data collection methods have been applied in the past. Chandler et al. (*3*), for example, used wire-linked vehicles to examine the responses of eight drivers in the following position, while Edie (*4*) tried to match his model to macroscopic data (*1*). More recently, data have been collected from driving simulators in the laboratory. The question about this approach, however, remains whether drivers behave the same way in a simulator as they do in reality.

Some researchers also collected data by observing vehicles from a position above the road. Ozaki, for example, gathered data by making use of video films taken from the 32nd floor of a city office building (*5*), whereas Treiterer and Myers mounted an aerial camera in a helicopter that took pictures at a mean interval of 1.0 s (they observed a platoon of about 70 vehicles during a time interval of 238 s) (*6*). One of the main advantages of the last two approaches is the ability to observe vehicles without influencing drivers.

The data set used for the study described in this paper has been derived from pictures of Freeway A2 in Utrecht, the Netherlands, taken from a helicopter, with intervals of 0.1 s between two successive images. During the observation, the helicopter remained (approximately) at the same position, which implies that a fixed part of the road with a length of 400 to 500 m, depending on the height of the

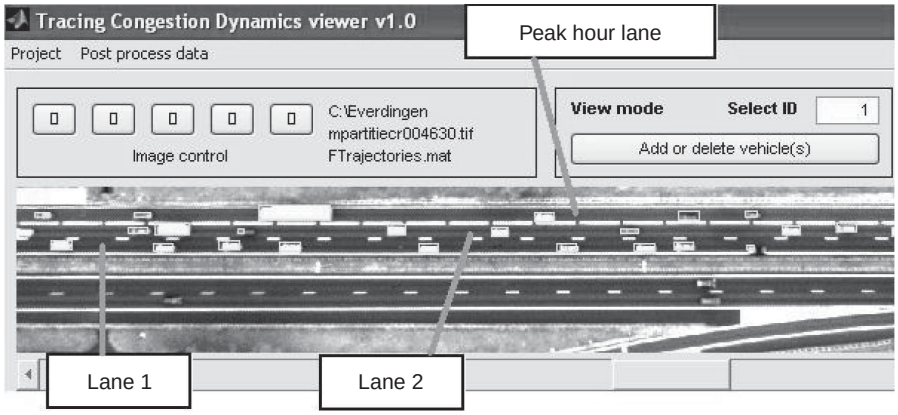

FIGURE 1 Vehicle viewer showing results of vehicle detection and tracking.

helicopter, was observed. The observation covers a time period of 300 s and is concerned with three lanes of the freeway (the upper three lanes in Figure 1). As one of these lanes was a peak hour lane (a lane that is used as an emergency lane in the off-peak hours and as an extra lane in the peak hours), it should be noted that the pictures are of an afternoon peak, implying that the traffic used all three lanes (including the peak hour lane).

Despite the introduction of this additional lane during the peak hours, it is still common on this part of the freeway for congestion to occur during the peak hours, as was also the case at the time of observation in the present study. This is illustrated in Figure 2 by taking a closer look at the average speeds of the cars on the road at each moment in time.

The pictures collected functioned as the input for a three-step procedure that resulted in the trajectory data needed for this paper:

Step 1. Dedicated software was used to detect individual vehicles within the pictures and to track them within a sequence of pictures, such that vehicle trajectories could be extracted. This process consists of several steps (for example, correction for lens distortion, radiometric correction, orthorectification and geocorrection, and determination of background images), as previously described in detail (*2*).

Step 2. The output of the software was manually checked by using a tool called the Tracing Congestion Dynamics (TCD) viewer. The TCD viewer (illustrated in Figure 1) uses the output of the software to draw for each time step boxes on the positions of vehicles. As the boxes are drawn in the original pictures, the user can check whether all vehicles are correctly detected and tracked. The tool also enables the deletion of false detections and incorrect tracking data from the output file. Furthermore, it offers the possibility of the manual detec-

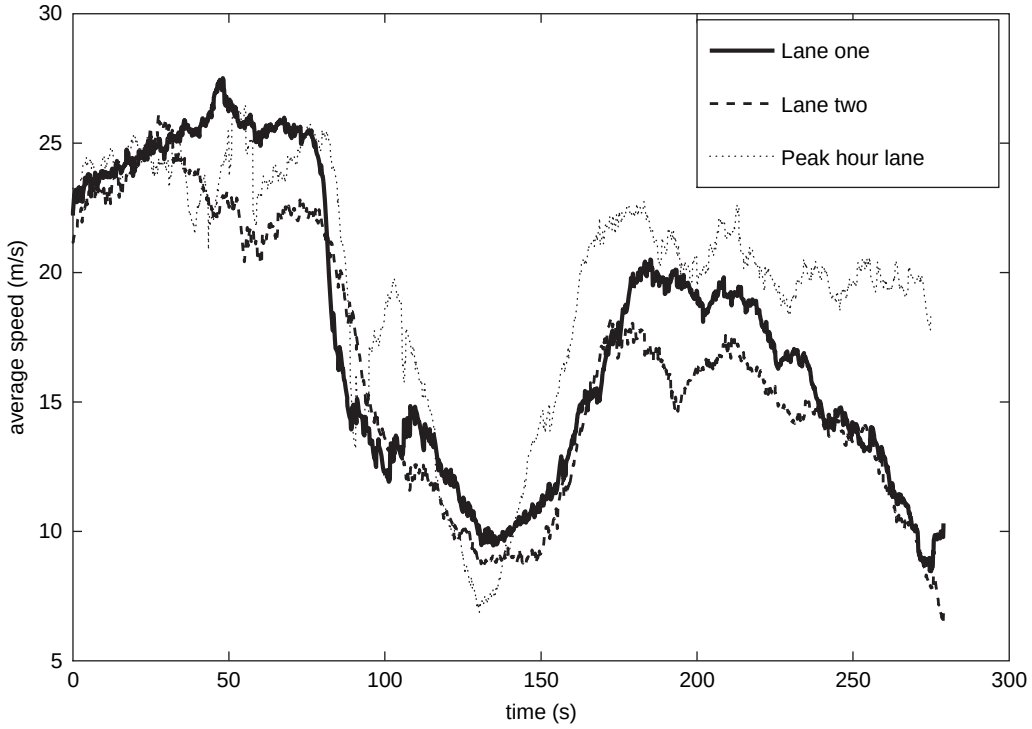

FIGURE 2 Space mean speeds on different lanes of the considered freeway.

tion of vehicles by allowing the user to draw a box around a vehicle in the picture, after which the tool automatically tracks the vehicle in subsequent pictures and adds the new vehicle to the output file.

Step 3. In the final step, special care was taken to address the fact that the data concerning the movements of the cars were derived from pictures. This implies that the accuracy of the data was 1 pixel (40 cm in real-life coordinates). To further improve the accuracy of the data, an iterative extended Kalman filter was applied to the data set, as described previously (*7*).

At the end of the procedure the following information was directly available for each vehicle (at 0.1-s intervals): the *x*-position of the vehicle and the *y*-position of the vehicle. Vehicle speeds in the *x*-direction as well as in the *y*-direction (first derivatives of the *x*- and *y*-trajectories), accelerations (second derivatives), lane distributions, and the order of the cars in each driving lane at intervals of 0.1 s were also derived.

Figure 2 shows the course of the space mean speeds during the period of observation. The space mean speed is easily determined from the trajectory data by taking the average speed of all vehicles present in the observed region at a certain instant in time. Figure 2 shows that the speeds decrease considerably after about 70 s. The speeds start to recover from time (*t*) 130 s onward but decrease slightly later again for Lanes 1 and 2.

SELECTING LEADER–FOLLOWER COMBINATIONS

To use these trajectory data for the proposed analysis of the GHR model, appropriate pairs of adjacent cars had to be selected. Three selection criteria were used:

1. The two cars had to be adjacent during the whole period during which they were both observed. If this was not the case, there was a lane change in which at least one of the vehicles was directly or indirectly involved. Because of this, it was reasoned that these vehicle pairs had to be excluded, as the following cars were not primarily occupied with following the leading car.
2. The period during which both cars were observed should have a length of at least 15 s (at least 150 observations).
3. The mean gross distance headway had to be shorter than 70 m, as it is assumed in the model that the driving behavior of the driver of the following car is dependent on the driver's observations of the car driving immediately in front. If, however, the distance between the two cars becomes too large, there will be no interaction. With respect to this criterion, it should be mentioned that the data were collected during a peak period that showed congestion. When the space mean speeds in Figure 2 are low, there are hardly any free drivers. When the speeds are higher, however, it is possible that not all drivers are in a following state. The threshold value for the mean gross distance headway of 70 m was based on a formula used to calculate a safe headway under the assumption that the braking distances of vehicles are nearly the same (*8*):

$$\text{safe distance headway } (t) = \text{overall reaction time} * v_f(t) + l_{sf} \quad (1)$$

where $v_f(t)$ is the speed of the following car at time t, and l_{sf} is the vehicle length plus the reserve safety distance at rest. If a vehicle length of 4.5 m and a reserve distance of 1 m are assumed and, furthermore, if a reaction time between 1 and 2 s at a speed of 25 m/s is assumed, the minimum safe distance is equal to 30.5 to 55.5 m. To ensure that all vehicles in the analysis are influenced by the preceding car, the threshold value for the mean distance headway was set to 70 m.

After application of these criteria, 128 pairs of vehicles were included in the analysis.

GHR MODEL

In the past many different modeling approaches have been used to describe the car-following behaviors of driver–vehicle combinations. Probably one of the most well-known models in this field is the GHR model, which is represented by the following equation:

$$a_f(t + T_r) = cv_f^m(t + T_r)\frac{\Delta v(t)}{\Delta x^l - (t)} \quad (2)$$

where

T_r = time between the observation of a certain stimulus and the reaction to that stimulus;
$a_f(t + T_r)$ = acceleration of the following vehicle at time $t + T_r$;
$v_f(t + T_r)$ = speed of following vehicle at time $t + T_r$;
$\Delta v(t)$ = relative speed between the car immediately in front and the following car ($v_{\text{leader}} - v_{\text{follower}}$);
$\Delta x(t)$ = relative distance between following car and car immediately in front ($x_{\text{leader}} - x_{\text{follower}}$); and
m, l, and c = parameters describing car-following behavior.

This model, which was introduced in 1961 (*9*), is actually a general form of earlier models. Chandler et al. (*3*), for example, presented a model equal to the special case of the GHR model in which both l and m were equal to 0, while Gazis et al. (*10*) introduced the model in which m was equal to 0 and l was equal to 1, and Edie (*4*) proposed a model in which both m and l were equal to 1.

A disadvantage of the model is its mechanistic character. For instance, the model requires drivers to react to arbitrarily small changes in the relative speed, even at very large spacings (*8*). It is also assumed that there is no response as soon as speed differences disappear.

One important aspect of the model nevertheless remains valuable: it defines factors that affect the acceleration of a following car. Thus, the mathematical relationship between the different stimuli and the acceleration defined above may be somewhat too rigid to describe all components of the complex behavior of human beings; nevertheless, it offers a good starting point in the determination of factors influencing following behavior.

DESCRIPTION OF MODELS ANALYZED

This paper analyzes the models that form the roots of the GHR model, which are presented below.

1. The model of Chandler et al. (*3*):

$$a_f(t + T_r) = cv_f^0(t + T_r)\frac{\Delta v(t)}{\Delta x^0(t)} = c\Delta v(t) \quad (3)$$

2. The model of Gazis et al. (*10*):

$$a_f(t + T_r) = cv_f^0(t + T_r)\frac{\Delta v(t)}{\Delta x^1 - (t)} = c\frac{\Delta v(t)}{\Delta x(t)} \quad (4)$$

3. The model of Edie (*4*):

$$a_f(t + T_r) = cv_f^1(t + T_r)\frac{\Delta v(t)}{\Delta x^1(t)} = cv_f(t + T_r)\frac{\Delta v(t)}{\Delta x(t)} \quad (5)$$

In the first model (Equation 3), it is assumed that the acceleration of the following car depends exclusively on the speed difference ($v_{leader} - v_{follower}$) between the cars. In the second model (Equation 4), an additional term is included, namely, the distance between the cars. This implies that a particular relative speed influences the acceleration of the following car more if the distance between the two cars is shorter. In the third model (Equation 5), it is assumed that the reaction of the following car depends not only on the speed difference and the relative distance but also on the speed of the following car.

PARAMETER ESTIMATION APPROACH

All three models considered in this paper are derived from the GHR model by choosing different values for the parameters *m* and *l*. The problem, then, is to estimate the remaining unknown parameters in the models, namely, *c* (the sensitivity parameters) and T_r (the reaction times), by using the data from the data set containing all necessary information about accelerations, relative speeds, relative distances, and speeds. In the proposed approach this will be achieved for each leader–follower combination individually in two steps.

In the first step the parameter *c* is estimated by performing a least-squares fit for a range of different reaction times (the smallest reaction time is 0.5 s and the largest one is 2 s, with steps in between of 0.1 s). Furthermore, each reaction time is tested to determine whether the estimated *c* is significant at the 5% level to establish whether there exists a relationship between the stimulus and the reaction $a_f(t + T_r)$. Next, the sum-of-squared errors and the estimates for *c* belonging to reaction times for which a significant relationship was found are stored. The reaction times for which no significant relationship was found are excluded from the analysis in Step 2.

Because consecutive observations of a single vehicle pair are being used, an autocorrelation most likely exists between the error terms, resulting in a violation of the conventional least-squares assumption. The major consequence of this is that application of the ordinary least-squares method leads to an underestimation of the sampling variance of the regression coefficient, *c*, resulting in an overestimation of the relevant *t*-statistic. More advanced statistical methods exist to handle this problem. It was decided, however, that for the sake of simplicity the conventional least-squares method would be used here but that the drawback of this method would be taken into account. This implies in practice that the conventional method is used but that more stringent requirements would be adopted in significance testing.

The second step in the analysis is comparison of the sum-of-squared errors between all reaction times for which *c* was found to be significant and to select the reaction time with the smallest sum-of-squared errors (if there existed at least one reaction time for which the parameter *c* was found to be significant).

For selection of the optimal T_r, the sensitivity of the sum-of-squared errors to changes in the values of T_r was found to be dependent on the leader–follower pair. As this was expected to cause an overestimation of the number of times that extreme values of T_r were optimal, it was decided to introduce a so-called Bayesian regulator in the objective function, such that the objective is given by

$$\min \sum_t \left[e(t)^2 + \gamma\left(T_r - T_r^*\right)^2\right] \quad (6)$$

where

T_r^* = a priori assumption about the optimal reaction time,
$e(t)$ = the error term for an observation [observed value of $a_f(t)$ minus the predicted value of $a_f(t)$], and
γ = a parameter that determines the degree to which the outcome is influenced by the introduction of the penalty term.

In this objective, T_r^* is set equal to 1.2 s, a value that is approximately in the middle of the broad range of different optimal reaction times suggested in earlier studies [the overview provided previously (*1*) indicates that many different optimal reaction times have been reported in the past]. Another reason for setting T_r^* equal to 1.2 s was a study of Herman and Potts that focused on the GHR model in which *m* was equal to 0 and *l* was equal to 1 (*11*). They reported an average reaction time of 1.2 s. The parameter γ was chosen to be sufficiently small to make sure that only the optimal T_r values for insensitive pairs were influenced.

When all models are finally calibrated separately for all leader–follower combinations, the results obtained from the different models can be compared to determine which model best fits the data for a certain leader–follower combination.

LEAST-SQUARES ANALYSES

The optimal values of *c* for separate leader–follower combinations were estimated by performing least-squares analyses for a range of different T_r values. Some results of these analyses are shown in Figures 3, 4, and 5 for Model 1, Model 2, and Model 3, respectively (all at reaction times of 1.1 s).

In Figures 3 to 5, there exists a relationship between the acceleration rate and the stimuli provided in the model. Figures 3 to 5 also show that the relationships defined by the different models are not able to give precise estimates of the values for $a_f(t + T_r)$, as a lot of scatter exists around the straight lines.

Tests for significance at the 5% percent level were also performed when the least-squares estimates were determined. As mentioned above, more stringent requirements for a parameter to be significant (the critical *t*-value was doubled) were adopted. A particular leader–follower combination was excluded from further analysis when there was no reaction time for which there was a significant relationship between the stimuli defined in the model and the acceleration rate. The results of these significance tests are provided in Table 1.

The results shown in Table 1 indicate that with these higher requirements there are 102 pairs for both Model 1 and Model 2 and 100 pairs for Model 3 for which a relationship was found, implying that a relation could be established for approximately 80% of the pairs (if the conventional *t*-value is used, there are only six pairs for Model 1, eight pairs for Model 2, and seven pairs for Model 3 for which no relation was found, which amounts to 5%, 6%, and 5% of all pairs considered, respectively). It is not possible to draw conclusions about the relative performance of the respective models from these numbers, as the differences between the models with regard to the numbers of pairs for which a relation was found are only very small.

DISTRIBUTIONS OF OPTIMAL PARAMETERS

In the development of a robust theory describing car-following behavior, it is important to take care of differences between drivers. Because little is known about the differences in car-following behaviors

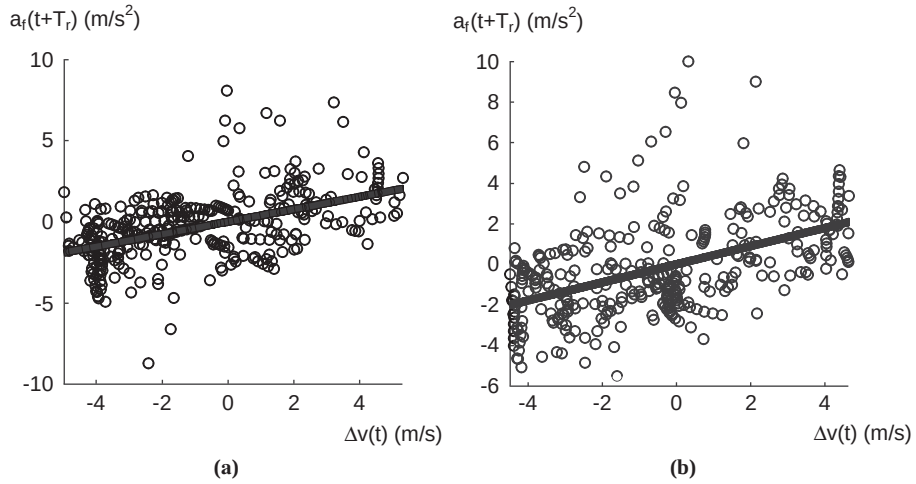

FIGURE 3 Least-squares estimates for sensitivity parameter c in Model 1 ($m = 0$, $l = 0$) for two different leader–follower combinations, both at reaction times of 1.1 s.

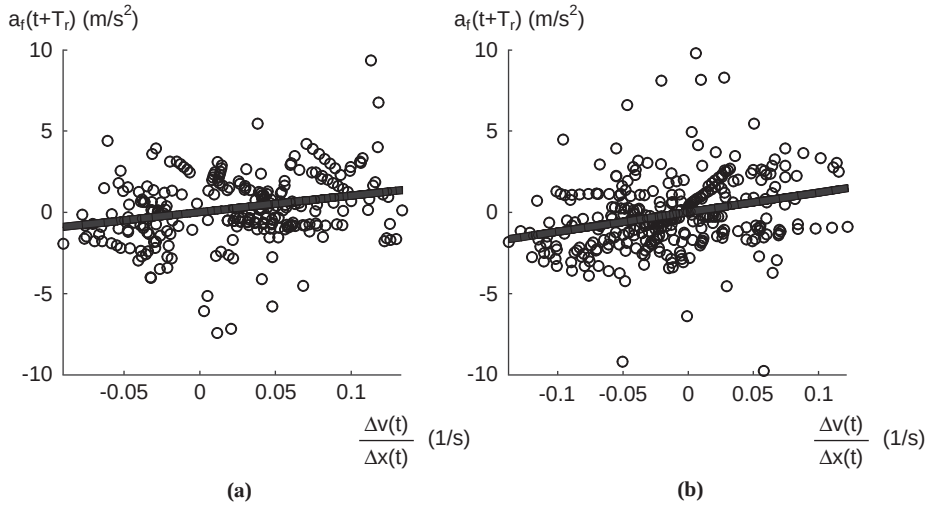

FIGURE 4 Least-squares estimates for sensitivity parameter c in Model 2 ($m = 0$, $l = 1$) for two different leader–follower combinations, both at reaction times of 1.1 s.

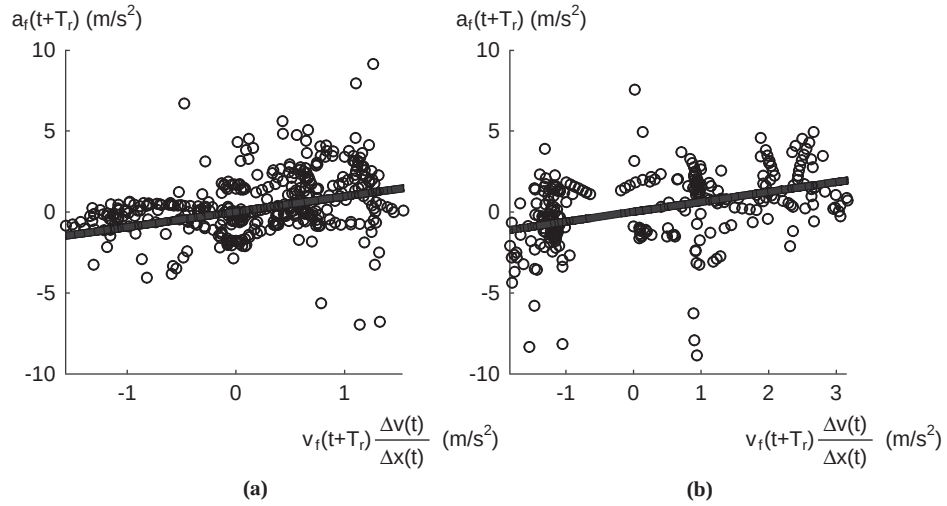

FIGURE 5 Least-squares estimates for sensitivity parameter c in Model 3 ($m = 1$, $l = 1$) for two different leader–follower combinations, both at reaction times of 1.1 s.

TABLE 1 Overview of Testing of Car-Following Relation

	Number of Pairs Available Before Testing for Significance	Number of Pairs Available After Testing for Significance		
		Model 1	Model 2	Model 3
All lanes	128	102	102	100
Lane 1	64	57	57	56
Lane 2	41	32	32	31
Peak hour lane	23	13	13	13

between individual drivers, the distributions of the estimated values for the parameters c and T_r are shown (Figures 6, 7, and 8 show these distributions for Model 1, Model 2, and Model 3, respectively). Table 2 summarizes the results of the analyses of the distributions.

The descriptive statistics in Table 2 show that considerable differences between different drivers (with regard to both the reaction time T_r and the sensitivity parameter c) could be identified. For example, a closer look at the estimates for the sensitivity parameter belonging to the first model shows that the estimates range from 0.18 to 0.83 s^{-1}. These specific values show a strong resemblance to the values reported by Chandler et al., as they found parameter values in the range of 0.17 to 0.74 s^{-1}, with an average value of 0.368 s^{-1} (*3*). The distributions of the optimal values for T_r in Figures 6, 7, and 8 show large peaks for T_r equal to 1.1 s (when T_r^* in Equation 6 was replaced by different values, for example, 1.8 and 0.8 s, this peak could also be observed at about 1.1 s).

COMPARISON OF MODELS

The last step in the analysis is to compare the results obtained with the different models. This analysis was done separately for all drivers. The model that best fit the data for each driver was first identified, and the difference (in percent) between the best model and the worst model (the best and the worst models are driver dependent) was then calculated.

After the results for all drivers were combined, it was found that the first and third models were each selected as the best one 36 times, while the second model best fit the data for 28 drivers. As the differences between these numbers are quite low, one model that outperformed the other models could not be selected from these results.

A closer look at the differences (in percent) between the performances of the best and the worst models (Figure 9) shows, on the one hand, that these differences are generally low. On the other hand, for some drivers the difference between the performances of the different models was considerable. As the optimal models for these drivers were different, there is some evidence that distinct drivers behave according to different car-following mechanisms.

CONCLUSIONS AND RECOMMENDATIONS

The car-following behaviors of individual drivers were studied by using vehicle trajectory data. These data were extracted from high-resolution digital images collected at a high frequency from a helicopter. The analysis was performed by estimating the parameters of different specifications of the well-known GHR car-following rule for individual drivers. The analysis showed that in 80% of the cases a relation between the stimuli (relative speed, relative distance, and

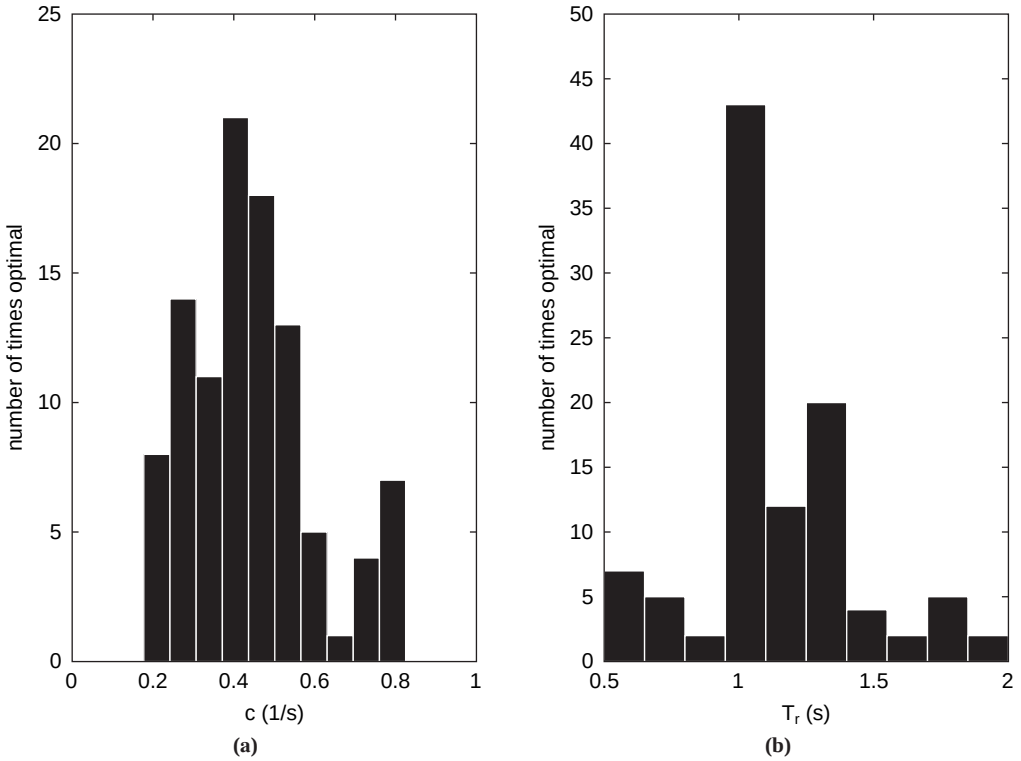

FIGURE 6 Distributions of optimal values for c and T_r (all lanes) for Model 1 ($m = 0$, $l = 0$).

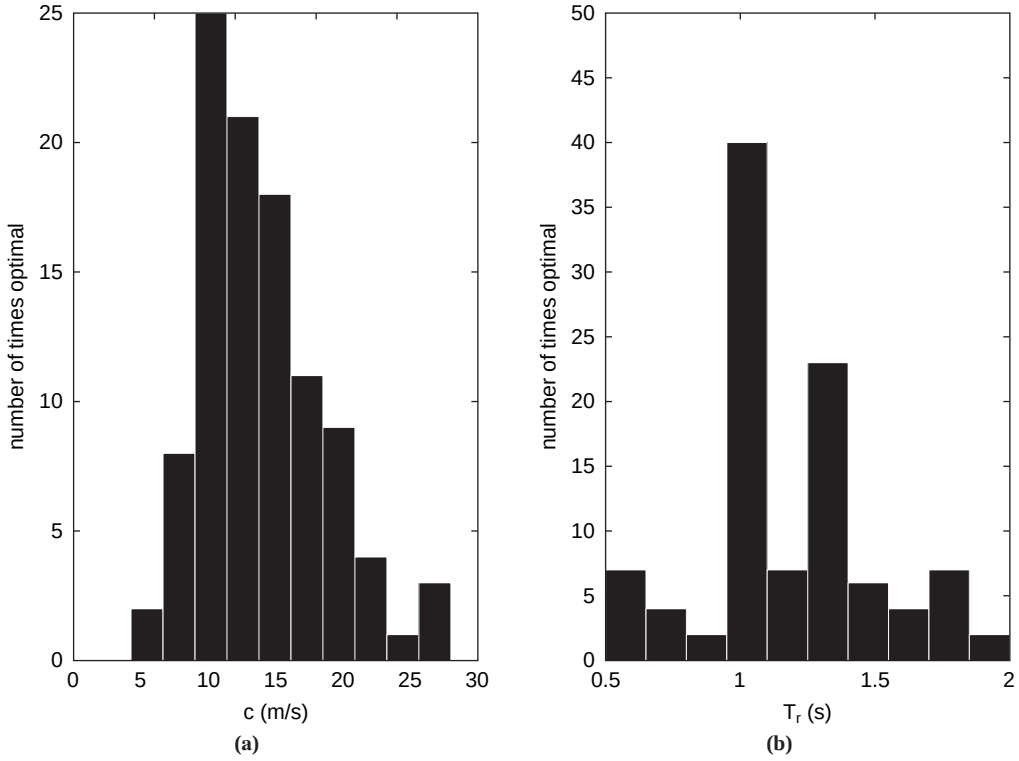

FIGURE 7 Distributions of optimal values for c and T_r (all lanes) for Model 2 ($m = 0$, $l = 1$).

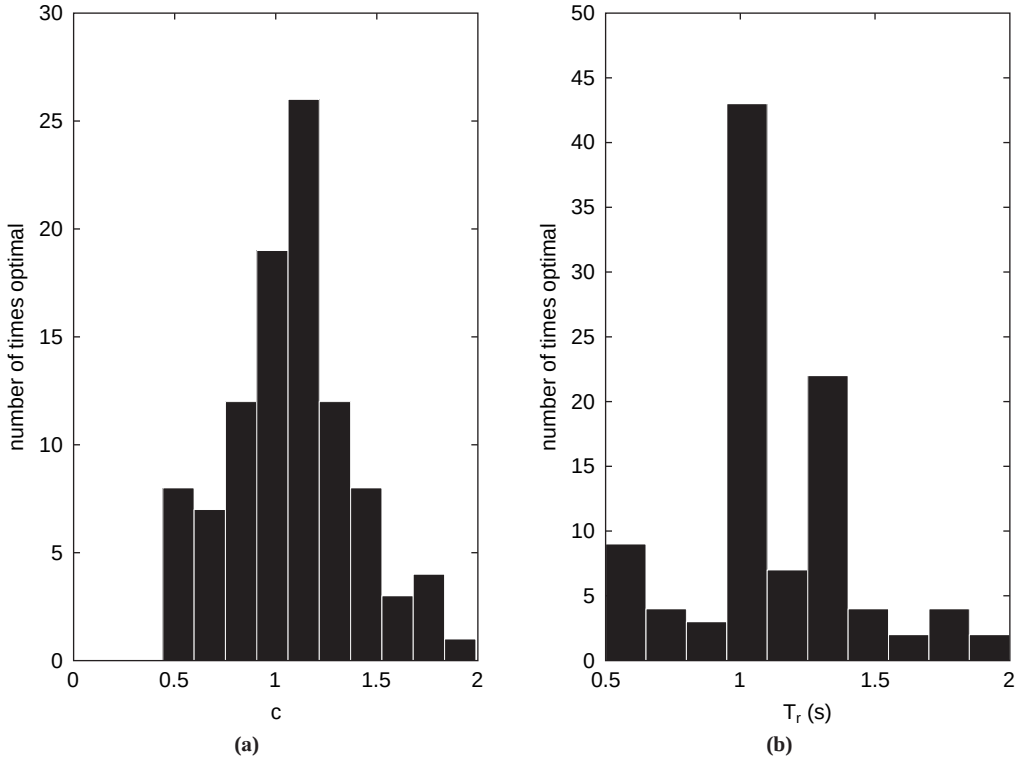

FIGURE 8 Distributions of optimal values for c and T_r (all lanes) for Model 3 ($m = 1$, $l = 1$).

TABLE 2 Overview of Descriptive Statistics for Distributions of T_r and c

		Reaction Time T_r		Sensitivity Parameter c	
		Mean	Standard Deviation	Mean	Standard Deviation
Model 1	All lanes	1.16570	0.2960	0.4400	0.1577
($m = 0, l = 0$)	Lane 1	1.1491	0.2959	0.4579	0.1571
	Lane 2	1.2063	0.2839	0.4343	0.1480
	Peak hour lane	1.1385	0.3380	0.3755	0.1774
Model 2	All lanes	1.2029	0.3123	14.0201	4.6949
($m = 0, l = 1$)	Lane 1	1.2105	0.3239	14.7262	4.4207
	Lane 2	1.2000	0.2712	12.5151	3.9971
	Peak hour lane	1.1769	0.3745	14.6284	6.6514
Model 3	All lanes	1.1540	0.3083	1.0795	0.3188
($m = 1, l = 1$)	Lane 1	1.1321	0.3169	1.1617	0.3167
	Lane 2	1.2194	0.2857	0.9691	0.2818
	Peak hour lane	1.0923	0.3201	0.9888	0.3288

the speed of the following car) and the response (acceleration of the following car) could be established.

The main contribution of this paper is that considerable differences between the car-following behaviors of individual drivers could be identified. These differences are expressed as different optimal parameter values for the reaction time and the sensitivity, as well as different car-following models that appear to be optimal on the basis of the data for individual drivers. This is an important result because most microscopic simulation models use a single car-following rule to predict traffic operations. Moreover, the result has implications for various characteristics of traffic flow, such as its stability.

The aim of future research is twofold. The first aim is to apply more advanced (statistical) methods that are better able to handle the problem of autocorrelated error terms and also to experiment with other car-following models. The second aim is to use larger data sets that consider different situations (roadway geometry, lane number, time of day, etc.). In the analysis of these data, particular attention will be paid to different kinds of traffic conditions and to whether or not adaptive car-following behavior can be established, as suggested by several researchers [for example, Dijker et al. (*12*)] to explain phenomena in congested traffic flow conditions that have remained inexplicable, until now.

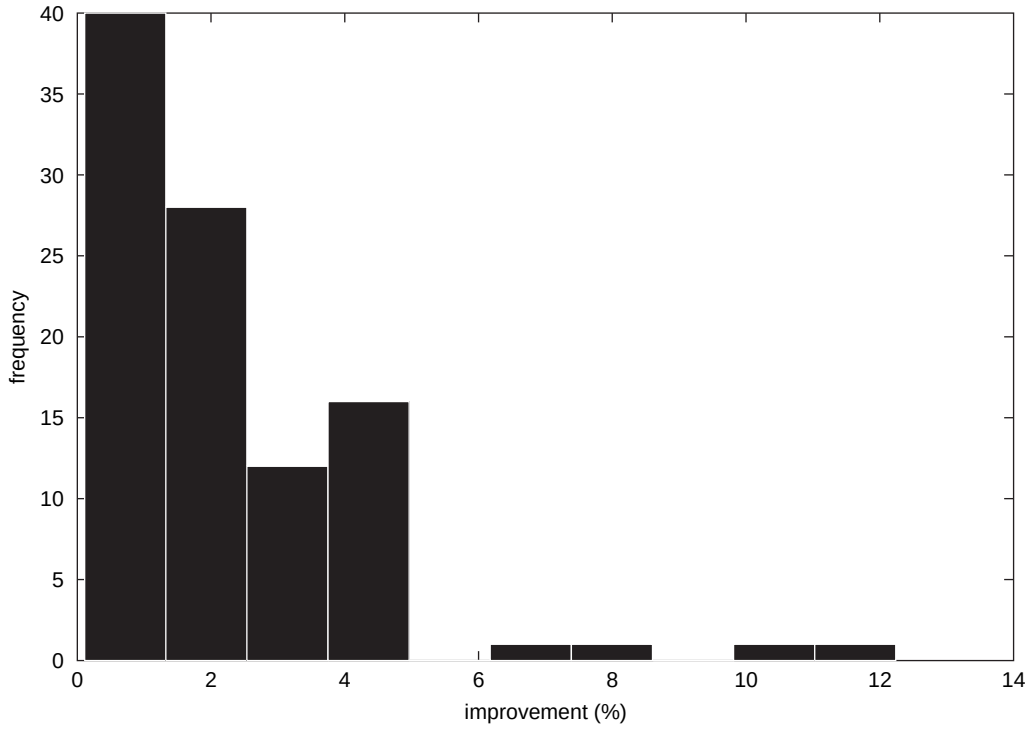

FIGURE 9 Improvement (in percentage) that can be achieved by using the best model instead of the worst model for all leader–follower combinations (choice of best and worst model is driver dependent).

ACKNOWLEDGMENT

The research is part of the research program Tracing Congestion Dynamics—with Innovative Traffic Data to a Better Theory, sponsored by the Dutch Foundation of Scientific Research (MaGW-NWO).

REFERENCES

1. Brackstone, M., and M. McDonald. Car-Following: A Historical Review. *Transportation Research, Part F,* Vol. 2, 1999, pp. 181–196.
2. Hoogendoorn, S. P., H. J. Van Zuylen, M. Schreuder, B. Gorte, and G. Vosselman. Microscopic Traffic Data Collection by Remote Sensing. In *Transportation Research Record: Journal of the Transportation Research Board, No. 1855,* Transportation Research Board of the National Academies, Washington, D.C., 2003, pp. 121–128.
3. Chandler, R. E., R. Herman, and E. W. Montroll. Traffic Dynamics: Studies in Car Following. *Operations Research,* Vol. 6, 1958, pp. 165–184.
4. Edie, L. C. Car Following and Steady State Theory for Non-Congested Traffic. *Operations Research,* Vol. 9, 1960, pp. 66–76.
5. Ozaki, H. Reaction and Anticipation in the Car Following Behavior. *Proc., 12th International Symposium on the Theory of Traffic Flow and Transportation* (C. F. Daganzo, ed.), Berkeley, Calif., Elsevier Science Publishers B.V., Amsterdam, Netherlands, 1993, pp. 349–366.
6. Treiterer, J., and J. A. Myers. The Hysteresis Phenomenon in Traffic Flow. *Proc., Sixth Symposium on Transportation and Traffic Flow Theory* (D. J. Buckley, ed.), Elsevier Scientific Publishing Company, Amsterdam, Netherlands, 1974, pp. 13–38.
7. Hoogendoorn, S. P., and H. J. Van Zuylen. Tracing Traffic Dynamics with Remote Sensing. In *Management Information Systems 2004: Incorporating GIS and Remote Sensing,* WIT Press, Southampton, United Kingdom, 2004, pp. 309–317.
8. Leutzbach, W. *Introduction to the Theory of Traffic Flow.* Springer-Verlag, Berlin, Germany, 1988.
9. Gazis, D. C., R. Herman, and R. W. Rothery. Nonlinear Follow-the-Leader Models of Traffic Flow. *Operations Research,* Vol. 9, 1961, pp. 545–567.
10. Gazis, D. C., R. Herman, and R. B. Potts. Car Following Theory of Steady State Traffic Flow. *Operations Research,* Vol. 7, 1959, pp. 499–505.
11. Herman, R., and R. B. Potts. Single Lane Traffic Theory and Experiment. *Proc., Symposium on Theory of Traffic Flow,* Research Labs, General Motors, 1959, pp. 147–157.
12. Dijker, T., P. H. L. Bovy, and R. G. M. M. Vermijs. Car-Following Under Congested Conditions: Empirical Findings. In *Transportation Research Record 1644,* TRB, National Research Council, Washington, D.C., 1998, pp. 20–28.

The Traffic Flow Theory and Characteristics Committee sponsored publication of this paper.